

Approaches for Estimating Liquefaction Potential of Soils

Vijay Kumar¹, Kumar Venkatesh², and Yeetendra Kumar³

^{1&3}Research scholars, Civil Engineering Department, Motilal Nehru national institute of technology, Allahabad, India, Pin-211004.

¹vijay03c34@gmail.com ³yeetendra@rediffmail.com

²Assistant professor, Civil Engineering Department, Motilal Nehru national institute of technology, Allahabad, India, Pin-211004. venkatesh@mnnit.ac.in

Abstract. In this paper, assessment of liquefaction of soils by various approaches have been reviewed and presented in chronological order. The study focuses on procedural requirements and assessment for conventional and computational methods. Simplified method given by Seed, Tokimatsu-Yoshimi (T-Y) and Idriss & Boulanger methods of liquefaction assessment have been analyzed. Computational methods like artificial neural network (ANN) and neuro-fuzzy technique (NF) is also discussed as capable in liquefaction assessment using database either from SPT or CPT results. Feed forward network with back propagation learning algorithm for ANN and TSK reliant NF has been evaluated. Conventional methods with extended application using concept of correction factors were induced in the analysis. Taking on familiarity from past literatures all methods were critically reviewed and measures are established.

Keywords: Liquefaction; Conventional method; Artificial Neural Network; Neuro-fuzzy; SPT

1 Introduction

Liquefaction is a phenomenon refers to the loss of strength in saturated, cohesion-less soils due to the buildup of pore water pressures under dynamic loading. Soil liquefaction generally occurs due to strong earthquake ground shaking where saturated cohesionless granular soil is transformed from a solid to a nearly liquid state. Soil liquefaction is generally occurs in sand, silty sand and sandy silt soil [1]. Following conditions are required for liquefaction to occur:

- The soils must be submerged below the water table.
- The soil must be loose/soft to moderately dense/stiff.
- The ground shaking must be intense
- The duration of ground shaking must be sufficient for the soils to lose their shearing resistance.

Majority of cohesive soil do not liquefy during earthquakes. In order to liquefy cohesive soil, it must meet the following criteria [2]:

- Percentage finer than 0.005mm should be <15%.
- The soil must have a liquid limit (LL) that is less than 35.
- The water content of the soil must be greater than 0.9 of the liquid limit i.e. $w > 0.9w_L$.

If the cohesive soil does not meet above three criteria, then it is usually considered not susceptible for liquefaction.

Cyclic laboratory and penetration tests on test models is used to determine potential for liquefaction for a given earthquake moment magnitude. Other than model tests state of art of liquefaction analysis envisages penetration test data and in-situ shear wave velocity for some of the semi-empirical procedures to estimate liquefaction potential. In view of involving test results along with analytical procedures the discussion is limited to renowned methods for creation of standard liquefaction charts.

2 Historical Development

2.1 SPT-N based analysis

The concept of critical SPT-N value (based on Niigata earthquake of 1964) for liquefaction assessment of sandy soil was first proposed by Koizumi (1966) and Kishida (1966) [3].

Owing to devastation from Japan earthquake Seed and Idriss [4] proposed frameworks for SPT-N-based assessments of liquefaction potential in simplified way. This procedure is time to time modified and improved by the researchers [2,4& 5]. An expert committee from National Research Council (NRC) of United States under the headship of Professor Robert V. Whitman evaluated the then existing methods of liquefaction assessment in 1985. Later National Centre for Earthquake Engineering Research (NCEEER) issued a report in 1997 but review continued till Youd and Idriss in 2001 published final recommendation on behalf of the committee which then became standard for liquefaction assessment. Other than councils, individual's efforts on state of art for evaluating liquefaction by own methods or for appraising limitations of existing methods continued, some of them are discussed in ongoing literature.

Tokimatsu and Yoshimi [6] carried out a study on sandy soil on past Niigata earthquake. Along with the developments of own charts he also used Seed's method.

Trifunac [7] carried out a study on fully saturated sand on the basis of five empirical equations developed from 90 case histories of liquefaction. Developed equation helped relating earthquake magnitude. Epicentral distance, site based motion of energy, peak ground velocity, Fourier amplitude of velocity and duration of motion with pore pressure.

Kayabali [8] and Andrus & Stokoe [9] carried out study on granular soil and soil ranging from fine sand to sandy gravel from 26 earthquakes on more than 70 sites respectively. They used Seed's and Seed's & Idriss method respectively, in addition new charts based on shear wave velocity data were developed for various earthquake magnitudes.

Lai et al [10] carried out a study on discriminant models from SPT of 592 datasets. He used two models which allowed calculated result to be compared to the empirical curves.

Rao and Satyam [11] prepared a liquefaction map of Delhi, India with the help of three empirical methods namely Seed and Idriss method; Seed and Peacock Method and Iwasaki method from 1200 boreholes at various locations along with geological and seismological details.

Arman and Kutunis [12] analyzed four well known methods namely simplified procedure, Tokimatsu and Yoshimi method, Seed-Dealba method and Japan Road Association method for Marmara earthquake in Turkey occurred on 17 august 1999 measuring 7.4 magnitudes.

2.2 Foundation of computational methods

To estimate liquefaction potential Goh, [13] developed a back propagation artificial neural network models with a typical transfer function i.e. "Sigmoid transfer function". Consequently in 2002 [14] Goh worked on probabilistic neural network (PNN) approach based on the well-established Bayesian classifier method, to evaluate seismic liquefaction potential. This paper demonstrate the usefulness of the PNN to model the complex relationship between the seismic and soil parameters, and the liquefaction potential using in situ measurements based on the CPT and the shear wave velocity.

Wang and Rahman [15] developed fuzzy artificial neural networks (FANN) for evaluation of liquefaction based on SPT-N value. He used two different databases in which $M, \sigma_o, \sigma'_o, a_{max}$, cyclic shear stress ratio, median grain diameter of the soil D_{50} ; critical depth of liquefaction D_{cr} , depth of water table D_w , were common parameters whereas SPT & CPT was exceptions, rather first database included fine content. Though numerous literatures are available but few significant parametric studies are discussed.

Hanna et al [16,17] explored GRNN methods to address collective knowledge from simplified procedures to assess nonlinear liquefaction potential. To meet this objective SPT and CPT results from 1999 Turkey and Taiwan earthquake were used. Further liquefaction decision was validated by the SPT, confirming the viability of the SPT to CPT data conversion which is the main limitation of most of the simplified methods.

Hsu et al [18] reported that high fines content (FC) and high cyclic stress ratio is the two main characteristics of the liquefied and non-liquefied cases in Taiwan. Field performance data generated from several earthquakes in Taiwan and gathered with previous records were used for SPT based models of neural networks.

Cha et al [19] established and compared single-artificial neural network (SANN) and multi-artificial neural network (MANN) models, and applied these models to predict wave induced liquefaction potential in a porous seabed. The results indicated accuracy of MANN model in the prediction of the wave-induced maximum liquefaction depth.

3 Estimation of Liquefaction Potential by Empirical Methods

Geotechnical professionals generally investigate subsurface to evaluate the potential for liquefaction. The most common techniques using standard penetration test (SPT) blow count (commonly referred as to the “N-value”) follows certain protocols:

1. Estimation of the cyclic stress ratio (CSR) induced at various depths within the soil by the earthquake.
2. Estimation of the cyclic resistance ratio (CRR) of the soil, i.e. the cyclic shear stress ratio which is required to cause initial liquefaction of the soil.
3. Evaluation of factor of safety against liquefaction potential of in situ soils.

3.1 Evaluation of Cyclic Stress Ratio (CSR)

3.1.1 Simplified procedure

After the disastrous earthquake in Alaska and Nigata (Japan) in 1964, Seed and Idriss [1] developed and published the basic, “simplified procedure”. The procedure is modified and improved periodically since the time, primarily through landmark papers by the researchers [5-6 & 20-21]. After 3 decades Youd et al. [22] again modified Seed’s method in laboratory held by NCEER and NSF. In this study these simplified procedures have been discussed below:

As per Newton’s 2nd law of motion, the horizontal earthquake force ‘F’ acting on the soil column has a unit width and length i.e.

$$F = ma = (W/g)a = (\gamma z/g)a_{\max} = \sigma_v(a_{\max}/g) \quad (1)$$

Where, F = horizontal earthquake force acting on soil column.

m = total mass of soil column i.e. (W/g) .

γ = total unit weight of soil

z = depth from the ground level

a = acceleration which in this case is maximum horizontal ground acceleration caused by the earthquake i.e. $a = a_{\max}$.

σ_v = total vertical stress at bottom of soil column.

g = acceleration due to gravity.

The force F acting on the rigid soil element is equal to the maximum shear force at the base on the soil element. Since the element is assumed to have a unit base width and length, the maximum shear force F is equal to the maximum shear stress as shown in fig 1.

$$\therefore \tau_{\max} = F = (a_{\max}/g)\gamma z \quad (2)$$

Since the soil column act as a deformable material rather than rigid body during the earthquake Seed and Idriss [4] incorporated a depth (or stress) reduction factor r_d in the right side, then the equation becomes

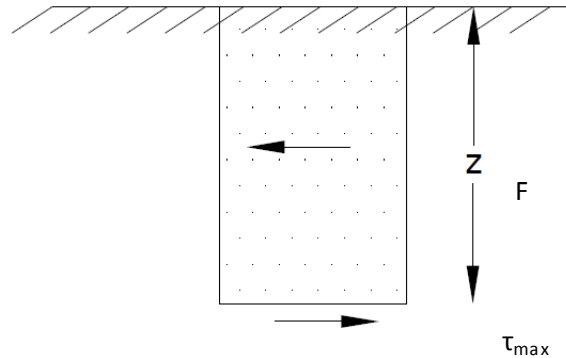


Fig. 1. Conditions assumed for evaluation of the CSR.

$$\tau_{max} = F = (a_{max}/g)\gamma z r_d \quad (3)$$

Average value of Stress reduction factor \$r_d\$ is given as:

$$r_d = 1.0 - 0.00765 z ; \text{ for } z \leq 9.15 \text{ m} \quad (4a)$$

$$r_d = 1.174 - 0.0267 z ; \text{ for } 9.15 \text{ m} < z \leq 23 \text{ m} \quad (4b)$$

$$r_d = 0.744 - 0.008 z ; \text{ for } 23 \text{ m} < z \leq 30 \text{ m} \quad (4c)$$

$$r_d = 0.50 ; \text{ for } z > 30 \text{ m} \quad (4d)$$

As depth (\$z\$) increases \$r_d\$ also increases. The mean value of \$r_d\$ calculated from above equation is shown in figure below.

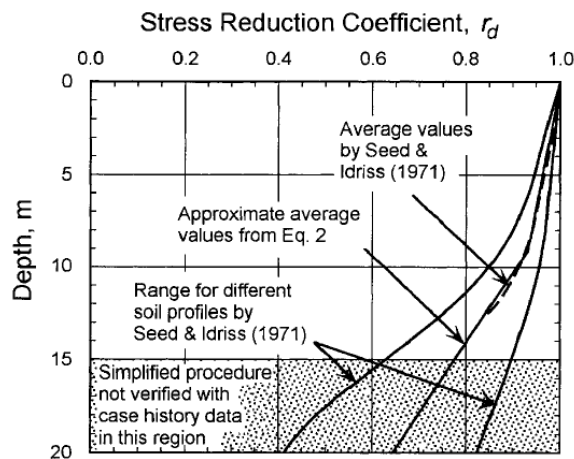


Fig. 2. \$r_d\$ versus depth curves (Youd and Idriss 2001).

For ease of computation, the mean value curve plotted in Fig 2 may be approximated by the following equation [22]:

$$r_d = \frac{(1.000 - 0.4113z^{0.5} + 0.04052z + 0.001753z^{1.5})}{(1.000 - 0.4177z^{0.5} + 0.05729z - 0.006205z^{1.5} + 0.001210z^2)} \quad (5)$$

For simplified method Seed et al [23] considered the soil in the field to undergo by average stress τ_{avg} , which is 0.65 of τ_{max} . Subsequently the average shear stress is normalized by the vertical effective stress to obtain CSR induced by the earthquake given in Eqn. (6):

$$CSR = \tau_{avg} / \sigma'_v = 0.65 (a_{max}/g) (\sigma_v / \sigma'_v) r_d \quad (6)$$

Where σ_v = total vertical stress
 σ'_v = total vertical effective stress ($\sigma_v - u$)
 u = pore water pressure.

3.1.2 Tokimatsu& Yoshimi (T-Y) method

On the basis of extensive laboratory test results of liquefaction on saturated sands, effects of seismic ground motions causing liquefaction may be represented by two quantities: horizontal ground acceleration and number of cycles of significant ground motions [6]. The finding is incorporated in the following equation for dynamic shear stress ratio for a given depth

$$\tau_{avg} / \sigma'_v = (a_{max}/g) \times (\sigma_v / \sigma'_v) r_d r_n \quad (7)$$

Where τ_{avg} = amplitude of uniform shear stress cycles equivalent to actual seismic shear stress time history.

a_{max} = The maximum horizontal acceleration at ground surface

σ'_v = initial effective vertical stress.

σ_v = initial vertical stress contribution to the shear stress, defined by

$$\sigma_v = \int_0^z \gamma dz \quad (8)$$

Where γ = unit weight of soil

And z = depth below the ground surface.

r_d and r_n are correction factors in terms of depth in and earthquake magnitude respectively and may be calculated as

$$r_d = 1 - 0.015z \quad (9a)$$

$$r_n = 0.1(M-1) \quad (9b)$$

On comparison of field behavior during earthquake of different magnitudes, the factor r_n in eq. (9b) is introduced so that a given number of cycles, N_1 of 0.65 times the maximum shear stress. Putting value of r_d and r_n in equation (7), CSR now defined as:

Table 1. Relationship among earthquake magnitude, number of cycles and r_n

Earthquake magnitude	No. of cycles	r_n
5.5	3	0.47
6.5	6	0.54
7.0	10	0.60
7.5	15	0.65
8.3	25	0.72

$$\tau_{avg}/\sigma_v' = 0.1(M - 1)(a_{max}/g)(\sigma_v/\sigma_v')(1 - 0.015z) \quad (10)$$

Where M = magnitude of earthquake.

3.1.3 Idriss & Boulanger's method

Modus operandi by Idriss & Boulanger [24] for evaluation of CSR is same as simplified method. Right after CSR calculated from the eqn. (6), value of CSR is adjusted for the moment magnitude $M = 7.5$. Accordingly the value of CSR is given as

$$(CSR)_{M=7.5} = CSR/MSF = 0.65 \left(\frac{\sigma_v a_{max}}{\sigma_v'} \right) \frac{r_d}{MSF} \quad (11)$$

A new parameter r_d which could be adequately expressed as a function of depth and earthquake magnitude (M) was introduced and may be explain from following relations:

$$\ln(r_d) = \alpha(z) + \beta(z)M \quad (12)$$

$$\alpha(z) = -1.012 - 1.126 \sin\left(\frac{z}{11.73} + 5.133\right) \quad (13a)$$

$$\beta(z) = 0.106 + 0.118 \sin\left(\frac{z}{11.28} + 5.142\right) \quad (13b)$$

Where z is the depth in meters and M is moment magnitude. These equations were approximated for depth $z \leq 34$ m however for depth $z > 34$ m; the following expression may be used:

$$r_d = 0.12 \exp(0.22M) \quad (14)$$

3.2. Evaluation of Liquefaction Resistance (CRR)

The cyclic resistance ratio (CRR) has been estimated by various researchers to estimate the liquefaction potential. The following well known methods have been described to adopt proper evaluation of CRR.

3.2.1 Youd's Method

Youd et al. [1] approximated the simplified base curve on fig. 3 using the following equation:

$$CRR_{7.5} = \frac{(a + cx + ex^2 + gx^3)}{(1 + bx + dx^2 + fx^3 + hx^4)} \quad (15)$$

Above equation is valid for $(N_1)_{60} > 30$ where $x = (N_1)_{60} > 30$ and is fixed at 1.20; $a = 0.048$; $b = -0.1248$; $c = -0.004721$; $d = 0.009578$; $e = 0.0006136$; $f = -0.0003285$; $g = -1.673E-05$ and $h = 3.714E-06$.

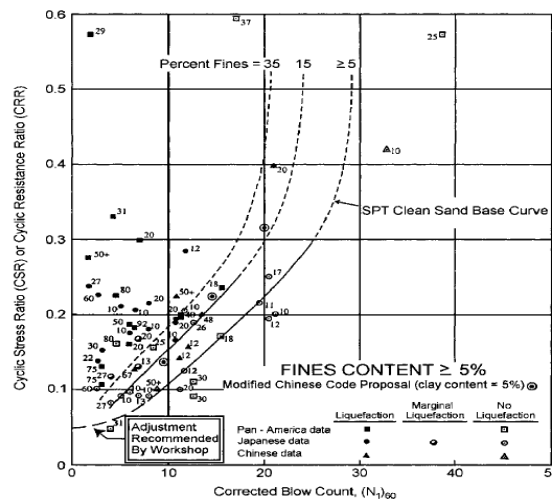


Fig. 3. CRR from SPT data along with empirical liquefaction data (Youd et al. 2001).

$CRR_{7.5}$ is the cyclic resistance ratio for magnitude of 7.5 earthquakes, magnitude smaller or larger than 7.5, introduces a correction factor namely magnitude scaling factor MSF defined by the following equation given by [1]:

$$MSF = 10^{2.24} / M^{2.56} \quad (16)$$

The appropriate cyclic strength obtained is:

$$CRR = (CRR_{7.5}) \times MSF \quad (17)$$

3.2.2 Tokimatsu and Yoshimi (T-Y) method

CRR specified by Tokimatsu and Yoshimi;

$$CRR = \tau_1 / \sigma'_v = a C_r \left[\left(16\sqrt{N_\alpha} / 100 \right) + \left(16\sqrt{N_\alpha} / C_s \right)^n \right] \quad (18)$$

Where τ_1 = shear stress on horizontal plane; C_r , a & n are correction factors and may be taken as 0.57, 14 & 0.45 respectively. N_α in eqn. (18) and subsequently N_1 , may be calculated from the following pairs of equations;

$$N_\alpha = \sqrt{N_1 + \Delta N_f} \quad (19a)$$

$$N_1 = C_N N = \frac{1.7}{\sigma'_o + 0.7} N \quad (19b)$$

Where ΔN_f is correction factor for SPT-N value and σ'_o is effective vertical stress. Tokimatsu and Yoshimi assumed $\Delta N_f = 0$ for clean sands and $\Delta N_f = 5$ for silty sands. Firat et al. [13] gave the value of ΔN_f as shown in table 2.

Table 2. Relation between fine content and correction factor for SPT-N value

Fines Content FC (%)	ΔN_f
0-5	0
5-10	interpolate
>10	0.1X FC +4

3.2.3 Idriss and Boulanger method

Idriss and Boulanger [22] adjusted the equation of CRR for clean sands as follows

$$CRR = \exp \left\{ \frac{(N_1)_{60cs}}{14.1} + \left(\frac{(N_1)_{60cs}}{126} \right)^2 - \left(\frac{(N_1)_{60cs}}{23.6} \right)^3 + \left(\frac{(N_1)_{60cs}}{25.4} \right)^4 - 2.8 \right\} \quad (20)$$

Subsequent expressions describes the way parameters in the above equation is calculated

$$(N_1)_{60cs} = (N_1)_{60} + (\Delta N_1)_{60} \quad (21a)$$

$$(\Delta N_1)_{60} = \exp \left(1.63 + 9.7/FC - (15.7/FC) \right) \quad (21b)$$

$$(N_1)_{60} = C_N (N)_{60} \quad (21c)$$

The variation of $(\Delta N_1)_{60}$ with FC, calculated using the eqn. (19c) is presented in fig. (3). The use of above equations provides a convenient means for evaluating the cyclic stress ratio required to estimate liquefaction for cohesion-less soils with varying fines content.

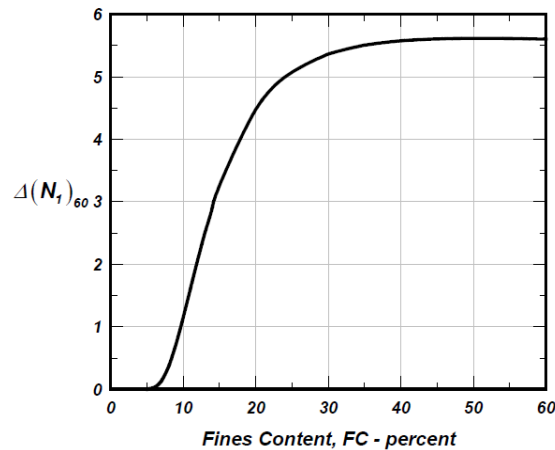


Fig. 4. variation of $(\Delta N_1)_{60}$ with fines content

3.3 Influence of MSF

According to Arango [24] MSFs are independent of acceleration, and are only dependent on the equivalent uniform number of stress cycles selected to represent different earthquake magnitude. According to Youd et al. [22], the magnitude scaling factors are commonly applied to CRR and equals 1.0 for earthquake with a magnitude of 7.5 for magnitudes other than 7.5 is shown in fig. 3.

3.3.1 Seed's scaling factor

In most cases, the magnitude scaling factors are commonly applied to CRR. The CRR curves in figure 3 apply only to magnitude 7.5 earthquakes. To adjust the CRR curves to magnitudes smaller and larger than 7.5, Seed and Idriss [20] introduced correction factors termed Magnitude Scaling Factors (MSF). This MSF is calculated from average number of loading cycles from various earthquake magnitudes. Further Seed et al. in 1984 revised set of MSF on based on laboratory shear test data as provided below in table 4.

3.3.2 Revised Idriss scaling factor

Presents magnitude scaling factors developed by various investigators. The 1996 NCEER workshop (Youd et al. 1997) recommended a range of factors that can be represented by

$$MSF = \left(\frac{M_w}{7.5} \right)^n \quad (22)$$

Where M_w = moment magnitude;
 and n = exponent.

Moment magnitude is the scale most commonly used for engineering applications and is preferred for liquefaction resistance calculations [1]. The lower bound for the range of MSF's recommended by the 1996 NCEER workshop is defined with $n = -2.56$. The upper bound of the recommended range is defined with $n = -3.3$ [9] for earthquakes with magnitude ≤ 7.5 . Magnitude scaling factor is defined by above equation and average r_d values originally proposed by Seed and Idriss [4] should be used together when evaluate CSR and CRR.

3.3.3 Idriss scaling factor

In recently past, Idriss (1999) proposed revised MSFs defined by

$$MSF = 6.9 \exp\left(-M_w/4\right) - 0.06 \quad (23)$$

This equation is valid for $M_w > 5.2$ for $M_w \leq 5.2$ take $MSF=1.82$. In addition, this equation is used for cyclic resistance ratio on earthquake magnitude 7.5. MSF for earthquakes to magnitude smaller or larger than 7.5, may be found through equation given by Youd et al.[22]:

$$MSF = 10^{2.24} / M^{2.56} \quad (24)$$

The appropriate cyclic strength is obtained by:

$$CRR = (CRR_{7.5}) \times MSF \quad (25)$$

3.3.4 Arango (1996) scaling factors

Arango (1996) developed two sets of MSF. The first set as given below was derived keeping in view the following parameters [25]:

- The farthest measured liquefaction from the seismic energy resources.
- The peak acceleration measured on aforesaid liquefaction site.
- Energy required causing liquefaction.

Table 3. Number of cycles by energy method

Earthquake magnitude M	Equivalent uniform number of cycles N_M
8.25	38.4
8	26.7
7.5	15
7	9.6

6	3.8
5.5	1.7

He gave a relationship between equivalent uniform number of cycles and MSF, which is expressed as:

$$MSF = \sqrt{15/N_M} \quad (26)$$

The second set of MSF (Table 4, column 4) was based on number of cycles that was proposed by Seed et al. 1985 and any field acceleration relationship suffered by liquefaction site.

3.3.5 Comparison of Magnitude Scaling Factors

Various MSFs values calculated by Seed et al. (1985), Arango (1996), Idriss (1999) and Youd et al. (2001) is shown below in table 4 consequently comparative graph between earthquake magnitude scaling factor is depicted in fig (5).

Table 4. Magnitude Scaling Factor Values Defined by Various Investigators

Magnitude (M)	Seed et al.	Arango Based on distant liquefaction site	Arango Based on number of cycles by Seed et al. 1975	Idriss	Youd et al.
1	2	3	4	5	6
5.5	1.43	3.00	2.20	2.21	1.68
6.0	1.32	2.00	1.65	1.77	1.48
6.5	1.19	1.60	1.40	1.44	1.30
7.0	1.08	1.25	1.10	1.19	1.14
7.5	1.00	1.00	1.00	1.00	1.00
8.0	0.94	0.75	0.85	0.85	0.87
8.25	----	0.63	----	0.78	0.82
8.5	0.89	----	----	0.73	0.76

3.4 Calculation of factor of safety

If the cyclic stress ratio caused by an earthquake is greater than the cyclic resistance ratio of the in situ soil, then liquefaction could occur during the earthquake, and vice versa. The factor of safety (FOS) against liquefaction is defined as:

$$FS_{Liquefaction} = CRR/CSR \quad (27)$$

Liquefaction is predicted to occur when $FS \leq 1.0$, and liquefaction predicted not to occur when $FS > 1$. The higher the factor of safety, the more resistant against

liquefaction [26], however, soil that has a factor of safety slightly higher than 1.0 may still liquefy during the earthquake.

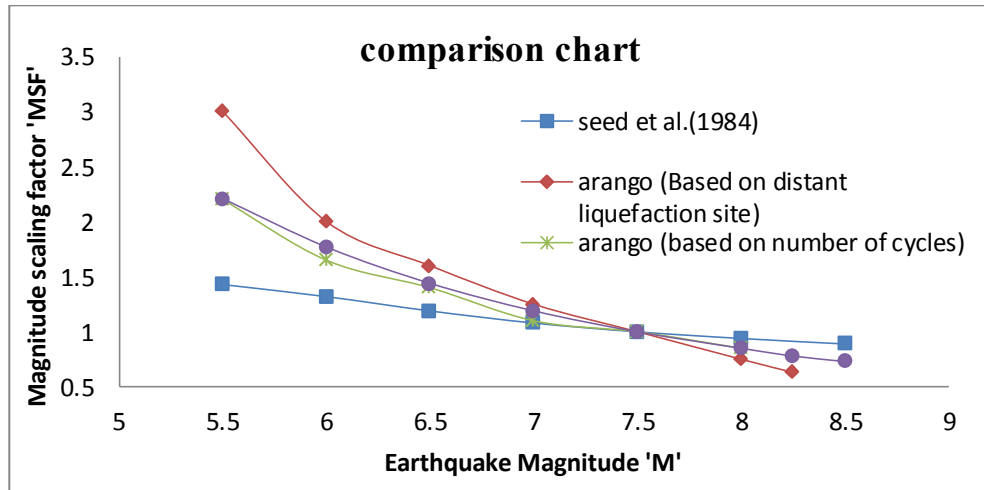


Fig. 5. Magnitude Scaling Factor values by different investigators.

4. Measures of liquefaction potential by computational methods:

4.1. ANN method

Artificial neural networks can be most adequately characterized as 'computational models' with particular properties such as the ability to adapt or learn, to generalize or to cluster or organize data and in which operation is based on parallel processing. Task of generalization is achieved by training and testing through division of input and target vectors into two datasets. An information processing unit may be understood by following diagram.

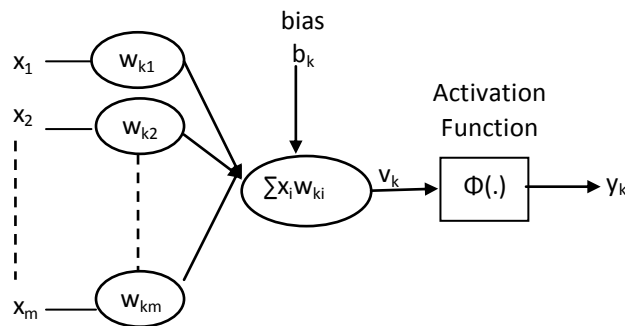


Fig. 6. A simple neuron in process.

Where x_1, x_2, \dots, x_m are input signals; $w_{k1}, w_{k2}, \dots, w_{km}$ are synaptic weights of neuron k ; u_k is the linear combiner output; b_k is the bias; $\phi(\cdot)$ is the activation function; v_k is the induced local field or activation potential; and y_k is the output signal [27]. The basic models of ANN may be specified by: synaptic interconnections; training or learning rules and the activation or transformation function. Using the above characteristics a number of model architecture may be prepared; one of them (feed forward network) with back propagation learning algorithm is described below.

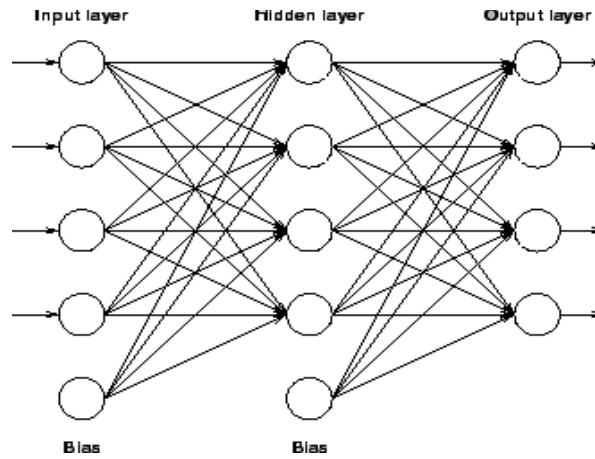


Fig.7. Back propagation neural network

The output from J^{th} node from hidden layer in fig 7.

$$o_j = \sum_{i=1}^n w_{ij} x_i + b_j \quad (28)$$

Where i & j presents input and hidden nodes respectively
 o_j is o/p from the j^{th} hidden node
 x_i is i/p introduced to node i
 w_{ij} is the synaptic weight on the link between i^{th} input and j^{th} o/p node
 b_j is the bias applied at the j^{th} hidden node

The activation function for the j^{th} hidden node may be determined using the sigmoid (or any other) function

$$v_j = \left[\frac{1}{1 + \exp^{-\sigma_j}} \right] \quad (29)$$

The o/p from the k^{th} node is obtained by:

$$o_k = \sum_{j=1}^n w_{jk} v_j + b_k \quad (30)$$

Where w_{jk} is the synaptic weight on the link between j^{th} hidden and k^{th} o/p node
 b_k is the bias applied at the k^{th} o/p node

The activation function v_k for the o/p node k is:

$$v_k = \left[\frac{1}{1 + \exp^{-o_k}} \right] \quad (31)$$

The error at the k^{th} o/p node is obtained by

$$\delta_k = (1 - v_k)(y_k - v_k)v_j \quad (32)$$

Correction to the weight on link between j^{th} hidden node and k^{th} o/p node during l^{th} iteration is

$$\nabla_{ljk} = \eta \delta_k v_j + \alpha_{(l-1)jk} \quad (33)$$

Where, $W_{(l-1)}$ is weight during (l-1) iteration

η is learning rate which determines the size of weight adjustment.

α is the momentum factor and used to change the weight by speeding up the convergence

Now updated weight is

$$w_{ljk} = w_{(l-1)jk} + \nabla_{ljk} \quad (34)$$

The correction ∇_{lk} applied to the bias b_k at o/p node k is

$$\nabla_{lk} = \eta \delta_k + \alpha b_{(l-1)k} \quad (35)$$

Where $b_{(l-1)k}$ is the bias applied at k^{th} o/p node during (l-1)th iteration

Updated bias on k^{th} o/p node during l^{th} iteration

$$b_{lk} = b_{(l-1)k} + \nabla_{lk} \quad (36)$$

The error value at j^{th} hidden node is

$$\delta_j = v_j(1 - v_j) \sum_{k=1}^n \delta_k w_{jk} \quad (37)$$

The correction to the weight on link between i^{th} i/p & j^{th} hidden node is

$$\nabla_{lij} = \eta \delta_j x_i + \alpha w_{(l-1)ij} \quad (38)$$

Updated weight on link between i^{th} & j^{th} o/p node is

$$w_{lij} = w_{(l-1)ij} + \nabla_{lij} \quad (39)$$

The correction to bias b_j applied at the hidden node j is

$$\nabla_{lj} = \eta \delta_j + \alpha b_{(l-1)j} \quad (40)$$

Where, $b_{(l-1)j}$ is bias applied at the j^{th} hidden node during $(l-1)^{\text{th}}$ iteration

Updated bias on j^{th} hidden node during l^{th} iteration is

$$b_{lj} = b_{(l-1)j} + \nabla_{lj} \quad (41)$$

This iteration continues until Mean Square Error reaches its minimum value.

4.2. Neuro-fuzzy Inference Method

An adaptive neuro-fuzzy inference system (ANFIS) structure simulates the fuzzy inference system (FIS). Fuzzy inference systems are mainly composed of a rule base, a database and a decision making unit [28]. The steps of FIS consist of fuzzification, allotment of membership grade, rule base development by employing if, then reasoning and finally defuzzification i.e. fuzzy set into crisp set. This is how an input variable x is fuzzified to be a partial member of the fuzzy set A by transforming it into a degree of membership of function $\mu_A(x)$ of interval $(0, 1)$ [29]. Though a number of neuro-fuzzy methods are available now a days, here most commonly used ANFIS structure containing zero order and first order Takagi-Sugeno-Kang (TSK) model are discussed with the help of figure 8 a, b.

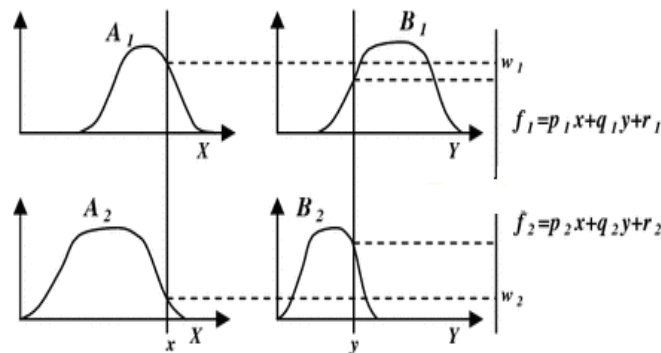


Fig.8(a).Sugeno method of fuzzy inference system

A typical rule in a Sugeno fuzzy model has the form, if input $x = A_1$ and input $y = B_1$, then output is given as

$$f_1 = p_1x + q_1y + r_1 \quad (42)$$

For a zero-order Sugeno model, the output level f_1 is a constant ($p_1 = q_1 = 0$). Likewise, If input $x = A_2$ and input $y = B_2$, then output is given as

$$f_2 = p_2x + q_2y + r_2 \quad (43)$$

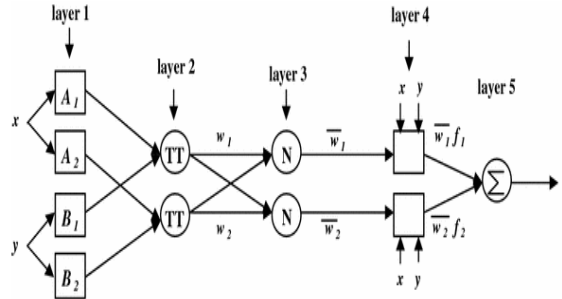


Fig.8(b).Architecture of ANFIS model in conjunction with Sugeno FIS

But if output f_1, f_2 are linear then we have first order TSK fuzzy inference system. The output level f_i of each rule is weighted by the firing strength w_i of the rule. For example, for an AND rule with input $x = A_i$ and input $y = B_i$, the firing strength is

$$w_i = \text{And Method } \{ \mu_{A_i}(x), \mu_{B_i}(y) \}, i=1,2$$

where, $\mu_{A_i}(\cdot)$ and $\mu_{B_i}(\cdot)$ are the membership functions for inputs 1 and 2. The final output of the system is the weighted average of all rule outputs, computed as shown in Equation 1 below

$$\text{Overall output} = \sum_i \bar{w}_i f_i = \frac{\sum_i w_i f_i}{\sum_i w_i} \quad (44)$$

5 Concluding Remarks

The SPT based liquefaction charts are commonly used for determining liquefaction potential. In general, advantages and disadvantages are always associated with discussed methods. Most of the assessment charts take Seed's method as the basis for determination of necessary factors. To estimate liquefaction potential gradual improvements in these methods made it more precise and viable for almost all kind of soils. Calculation of CSR, CRR and MSF require necessary assumption on early stages, alternatively computational models may save time by omitting lengthy and tedious task of calculation of aforementioned parameters. Some pertinent soil properties along with seismic characteristics may help in modeling and analyzing liquefaction potential of prone sites. The major advantage of computational methods is the ability to associate both SPT and CPT indicator properties for better engineering judgment to evaluate site dependent liquefaction. The rational approach to estimate

liquefaction potential will be useful for design and construction of civil engineering structures.

Acknowledgements

Authors are indebted to Dr. R. P. Tiwari for his patron ship and valuable contribution in collecting pertinent datasets hence facilitate in exploring further possibilities in this area of research.

References

1. Youd, T.L., Idriss, I.M., Summery Report on NCEER Workshop on Evaluation of Liquefaction Resistance of Soils, Nat. Ctr. for Earthquake Engg. Res., State Univ. of New York, Buffalo (1997).
2. Seed, H.B., Idriss, I.M., Arango, I. Evaluation of Liquefaction Potential using Field Performance Data. *J. Geotech. Engg.*, 09(3), 458--482 (1983).
3. Choobbasti, A.J., Firouzian, S.: Assessment of Cyclic Resistance Ratio of Babolsar Sandy Soil based on Semi-Empirical Relationships. *International J. of Resea. and Rev. in Apd. Scs.* 2(1), 9--16 (2010).
4. Seed, H.B., Idriss, I.M.: Simplified Procedure for Evaluating Soil Liquefaction Potential. *J. Soil Mech. and Found. Div.* 97(9), 1249--1273 (1971).
5. Seed, H.B.: Soil Liquefaction and Cyclic Mobility Evaluation for Level Ground During Earthquakes. *J. Geotech. Engg. Div.* 105(2), 201--255 (1979).
6. Tokimatsu, K., Yoshimi, Y.: Empirical Correlation of Soil Liquefaction Based on SPT-N Values and Fines Content. *Soils Found. JSSMFE.* 23(4), 56--74 (1983).
7. Trifunac, M.D.: Empirical Criteria for Liquefaction in Sands via Standard Penetration Tests and Seismic Wave Energy. *Soil Dyn. and Earth. Engg.* 14, 419--426 (1995).
8. Kayabali, K.: Soil Liquefaction Evaluation using Shear Wave Velocity. *Engg. Geology.* 44, 121--127 (1996).
9. Andrus, R.D., Stoke, K.H.: Liquefaction Resistance of Soils from Shear-Wave Velocity. *J. Geotech. Engg. ASCE* 111(12) (2000) 1015--1025.
10. Lai, S.Y., Lin, P.S., Hsieh, M.J., Jim, H.F.: Regression Model for Evaluating Liquefaction Potential by Discriminant Analysis of the SPT N value. *Can. Geotech. J.* 42, 856--875 (2005).
11. Rao, K.S., Satyam, D.N.: Liquefaction Studies for Seismic Microzonation of Delhi Region. *Current Science.* 92(5), 646--654 (2007).
12. Firat, S., Arman, H., Kutanis, M.: Assessment of Liquefaction Susceptibility of Adapazari City after 17th August, 1999 Marmara Earthquake. *Scientific Research and Essay.* 4(10), 1012--1023 (2009).
13. Goh, A.T.C.: Seismic Liquefaction Potential Assessed by Neural Networks. *J. of Geot. Engg.* 120 (9), 1467--1480 (1995).
14. Goh, A.T.C.: Probabilistic Neural Network for Evaluating Seismic Liquefaction Potential. *Can. Geotech. J.* 39, 219--232 (2002).
15. Wang, J., Rahman, M.S.: A Neural Network Model for Liquefaction-Induced Horizontal Ground Displacement. *Soil Dyn. and Earth. Engg.* 18, 555--568 (1999).
16. Hanna, A.M., Ural, D., Saygili, G.: Neural Network Model for Liquefaction Potential in Soil Deposits using Turkey and Taiwan Earthquake Data. *Soil Dyn. and Earth. Engg.* 27, 521--540 (2007a).

17. Hanna, A.M., Ural, D., Saygili,G.: Evaluation of Liquefaction Potential of Soil Deposits using Artificial Neural Networks,Int. J. for Comp.Aaid. Engg and Soft. 24(1),5--16 (2007b).
18. Hsu, S.C.,Yang, M.D., Chen, M.C., Lin, J.Y.:Artificial Neural Network of Liquefaction Evaluation for Soils with High Fines Content.International Joint Conference on Neural Networks, pp. 264--2649.Canada (2006).
19. Cha, D., Zhang, H. Blumenstein, M.: Prediction of Maximum Wave-Induced liquefaction in Porous seabed using Multi-Artificial Neural Network Model. Ocean Engineering,38, 878--887(2011).
20. Seed, H.B., Idriss, I. M.:Summer Report on Ground Motions and Soil Liquefaction during Earthquakes. Earthquake Engineering Research Institute. Berkeley, California (1982).
21. Seed, H.B., Tokimatsu, K., Harder, L. F., Chung, R. M.:The Influence of SPT Procedures in Soil Liquefaction Resistance Evaluations.J. Geotech. Engg., 111(12), 1425--1445 (1985).
22. Youd et al.:Liquefaction Resistance of Soils. Summary Report from the 1996 NCEER and 1998 NCEER/NSF Workshops on Evaluation of Liquefaction Resistance of Soils.J. Geotech. andGeoenv. Engg.127(10), 817--833 (2001).
23. Seed et al., Summery Report on Influence of seismic history of the liquefaction characteristics of sands, Earthquake Engineering Research Institute, Berkeley, California. Report no. EERC 75-25 (1975).
24. Idriss, I.M., Boulanger, R.W.:Semi-empirical Procedures for Evaluating Liquefaction Potential during Earthquakes.Soil Dyna.and Earth. Engg.26, 115--130 (2006).
25. Arango, I.:Magnitude Scaling Factors for Soil Liquefaction Evaluations.J. Geotech. Engg.122(11),929--936 (1996).
26. Lee, W.H.K., Kanamori, H., Jennings, P.C., Kisslinger, C.:International Handbook of Earthquake and Engineering Seismology. Part B. Aacademic Press, UK(2003).
27. Haykin, S.: Neural Networks, 2nd Ed., Prentice Hall, New Delhi, India(2006).
28. Habibagahi,G.: Post Construction Settlement of Rockfill Dams Analyzed via Adaptive Network based Fuzzy Inference System, J. of Comp. and Geotec.29, 211--233 (2002).
29. Shahin, M.A., Maier, H.R., Jaksa, M.B.: Settlement Prediction of Shallow Foundation on Granular Soils using B-spline NeuroFuzzy Models. J. of Comp. and Geotech.29, 211-233 (2003).